LDH-A inhibition, a therapeutic strategy for treatment of hereditary leiomyomatosis and renal cell cancer

Han Xie,[1] Vladimir A. Valera,[3] Maria J. Merino,[4] Angela M. Amato,[2] Sabina Signoretti,[2] William M. Linehan,[3] Vikas P. Sukhatme,[1] and Pankaj Seth[1]

[1]Department of Medicine, Division of Interdisciplinary Medicine and Biotechnology, Beth Israel Deaconess Medical Center, Harvard Medical School; [2]Department of Pathology, Brigham and Women's Hospital, Boston, Massachusetts and [3]Urologic Oncology Branch and [4]Laboratory of Pathology, Center for Cancer Research, National Cancer Institute, NIH, Bethesda, Maryland

Abstract

The genetic basis for the hereditary leiomyomatosis and renal cell cancer syndrome is germ-line inactivating mutation in the gene for the Krebs/tricarboxylic acid cycle enzyme, fumarate hydratase (FH), the enzyme that converts fumarate to malate. These individuals are predisposed to development of leiomyomas of the skin and uterus as well as highly aggressive kidney cancers. Inhibition of FH should result in significant decrease in oxidative phosphorylation necessitating that glycolysis followed by fermentation of pyruvate to lactate will be required to provide adequate ATP as well as to regenerate NAD^+. Moreover, FH deficiency is known to up-regulate expression of hypoxia-inducible factor (HIF)-1α by enhancing the stability of HIF transcript. This leads to activation of various HIF-regulated genes including vascular endothelial growth factor and glucose transporter GLUT1 and increased expression of several glycolytic enzymes. Because lactate dehydrogenase-A (LDH-A), also a HIF-1α target, promotes fermentative glycolysis (conversion of pyruvate to lactate), a step essential for regenerating NAD^+, we asked whether FH-deficient cells would be exquisitely sensitive to LDH-A blockade. Here, we report that hereditary leiomyomatosis and renal cell cancer tumors indeed overexpress LDH-A, that LDH-A inhibition results in increased apoptosis in a cell with FH deficiency and that this effect is reactive oxygen species mediated, and that LDH-A knockdown in the background of FH knockdown results in significant reduction in tumor growth in a xenograft mouse model. [Mol Cancer Ther 2009;8(3):626–35]

Introduction

Many cancer cells show enhanced glycolysis (1). In recent years, the molecular basis for this effect has started to be elucidated. In particular, up-regulation of hypoxia-inducible factor (HIF), which occurs as a consequence of hypoxia as well as from alterations in certain oncogenes or mutations in tumor suppressor genes, results in the increased transcription of genes involved in glucose transport, glucose metabolism, lactate formation, and lactate export from cells (2–6). Moreover, HIF activation results in decreased activity of the pyruvate dehydrogenase complex (7, 8). Collectively, these studies provide a partial explanation for the Warburg effect, which states that, even under aerobic conditions, cancer cells preferentially undergo glycolysis followed by fermentation (9). Fumarate hydratase (FH) plays an important role in the mitochondrial tricarboxylic acid cycle by catalyzing the conversion of fumarate to malate. The primary function of the Krebs/tricarboxylic acid cycle is oxidation of pyruvate to generate ATP. The genetic basis for the hereditary leiomyomatosis and renal cell cancer (HLRCC) syndrome is germ-line inactivating mutation in the FH gene (10–12). Inhibition of FH and presumably of oxidative phosphorylation should necessitate that fermentative glycolysis will be required to provide ATP as well as regenerate NAD^+ for glycolysis. The pseudohypoxic drive in HLRCC involving fumarate-dependent HIF activation as a result of competitive HIF prolyl hydroxylase inhibition by accumulated fumarate is likely to lock FH-deficient cells into a glycolytic pathway for sustaining the metabolic energy requirements (13).

In the present study, we wanted to ask whether FH-deficient cells do rely on glycolysis for growth and/or proliferation and whether they would be sensitive to inhibition of fermentative glycolysis. The fermentative reaction is regulated by lactate dehydrogenase (LDH), which in most tissue occurs in two major isoforms LDH-A and LDH-B. LDH-B is a homotetramer of LDH-H and favors the conversion of lactate to pyruvate and is also known to be up-regulated in many cancers (14). LDH-A is a heterotetramer of LDH-M and favors conversion of pyruvate to lactate and is up-regulated in many solid tumors that have high HIF expression (3, 15). LDH-A is an attractive target for cancer therapy because its expression is largely relegated to skeletal muscle. It is not present in red cells, in which glycolysis

Received 11/10/08; accepted 12/20/08; published OnlineFirst 3/10/09.

Grant support: National Cancer Institute Temin award K01 CA104700 (P. Seth), Dana-Farber/Harvard Cancer Center Kidney Cancer Specialized Program of Research Excellence (P. Seth, H. Xie, A.M. Amato, S. Signoretti, and V.P. Sukhatme), and National Cancer Institute, NIH contract N01-C0-12400 (V.A. Valera, M.J. Merino, and W.M. Linehan).

The costs of publication of this article were defrayed in part by the payment of page charges. This article must therefore be hereby marked *advertisement* in accordance with 18 U.S.C. Section 1734 solely to indicate this fact.

Requests for reprints: Pankaj Seth, Department of Medicine, Division of Interdisciplinary Medicine and Biotechnology, Beth Israel Deaconess Medical Center, Harvard Medical School, Dana 5 RW 561, 330 Brookline Avenue, Boston, MA 02215. Phone: 617-667-2029; Fax: 617-667-7581. E-mail: pseth@bidmc.harvard.edu

doi:10.1158/1535-7163.MCT-08-1049

followed by fermentation is an obligatory process for energy generation. Moreover, it is well known that humans with LDH-A deficiency only show myoglobinuria under intense anaerobic exercise (16, 17) and individuals with complete lack of LDH-A or LDH-B subunit have been documented with no apparent increase in hemolysis (16, 18, 19). Therefore, it is likely that potential LDH-A inhibitors might show relatively modest systemic toxicity.

Materials and Methods

Patient Samples and Characteristics: HLRCC and von Hippel-Lindau Phenotypic/Genotypic Assessment and Tumor Sample Procurement

Patients with suspected or confirmed HLRCC and von Hippel-Lindau (VHL) were evaluated in the Urologic Oncology Branch of the National Cancer Institute, where they underwent a comprehensive clinical evaluation for phenotype assessment. Each of the 10 patients with HLRCC-associated kidney cancer came from a family with confirmed FH germ-line mutation: 6 had surgery at the National Cancer Institute and the other 4 had surgery at outside institutions. The clear cell kidney cancers came from VHL patients with confirmed germ-line mutation of the VHL gene; all 6 had kidney cancer surgery done at the National Cancer Institute. The LDH-A staining in VHL and HLRCC tumor samples was compared with nonmalignant kidney tissue. The pathology of all of the renal tumors was reviewed by coauthor M.J.M.

Immunohistochemistry

Slides (5 μm) form formalin-fixed, paraffin-embedded tissue samples were used for immunohistochemistry. Slides were deparaffinized in three changes of xylene for 5 min each followed by rehydration in graded alcohols. Antigen retrieval was achieved by heating the slides in Tris-EDTA (pH 9.0) in a microwave oven at 95°C for 20 min. Endogenous peroxidase activity was inhibited by incubation in 3% hydrogen peroxide in methanol for 10 min. Sections were then incubated for 1 h at room temperature with sheep anti-human LDH-A antibody (1:30,000; Abcam) or isotype-matched IgG as negative controls. After several washes in Tris, samples were further incubated with rabbit anti-sheep IgG (1:1,000; Millipore) as a secondary antibody for 30 min at room temperature. Slides were then incubated with goat anti-rabbit horseradish peroxidase polymer (Envision PO System; DAKO) for 30 min followed by 3,3′-diaminobenzidine as chromogen for 5 min. The sections were counterstained with Mayer's hematoxylin and permanently mounted. Staining for LDH-A in HLRCC and VHL-null tumors was evaluated in four high-power fields and samples were scored as strongly positive (3+), moderately positive (2+), weakly positive (1+), or negative (0). Staining pattern (membranous, cytoplasmic, or nuclear) was also recorded.

Chemicals and Reagents

Cell culture medium was purchased from the American Type Culture Collection. Lentiviral short hairpin RNA (shRNA) constructs were purchased from Sigma-Aldrich, and the viral power kit and packaging cell line 293FT were purchased from Invitrogen. Sheep polyclonal LDH-A antibodies were purchased from Abcam, and FH mouse monoclonal was purchased from Novus. Rabbit polyclonal for activated caspase-3 and activated poly(ADP-ribose) polymerase (PARP) were purchased from Cell Signaling. The assay kit for measuring ATP was purchased from Roche. Lactate measurement kit was purchased from CMA microdialysis. Cell cycle reagents and Annexin V assay kits were purchased from Guava Technologies. Athymic mice for tumor implantation were purchased from Charles River Laboratories. A549 cells were maintained in Ham's F-12 with glutamine and sodium pyruvate with 10% FCS (Sigma). RCC4 and RCC4 + VHL cells were gift from Celeste Simon (University of Pennsylvania School of Medicine). Sequences of shRNA used in this study were LDH-A CCACCATGATTAAGGGTCTTT, LDH-A1 GATCTGTGATTAAAGCAGTAA, FH63 CGCTGAAGTAAACCAGGATTA, and FH65 CCCAACGATCATGTTAATAAA.

Generation of FH-, LDH-A-, and FH/LDH-A-Deficient Cell Lines

A549 cells were infected separately with empty shRNA vector control, three different FH shRNAs, and LDH-A lentiviral particles as described (20). Briefly, Recombinant lentiviral particles were produced by transient transfection of 293T cells according to standard protocol. Briefly, subconfluent 293FT cells were cotransfected with 3 μg shRNA plasmid and 9 μg viral power packaging mix (an optimized proprietary mix of three plasmids, pLP1, pLP2, and pLP/VSVG; Invitrogen) using Lipofectamine 2000 (Invitrogen). After 16 h, culture medium was switched to regular growth medium and cells were allowed to incubate for additional 48 h. Conditioned cell culture medium containing recombinant lentiviral particles was harvested and frozen. A549 cells were treated with above cell culture supernatant containing lentiviral particles for 24 h. These cells were then selected in puromycin (Sigma-Aldrich) to generate stable cell lines encoding empty vector, FH, and LDH-A shRNA. The selected cell lines were validated for diminished LDH-A and FH expression by Western blot analysis. Briefly, total cellular proteins were separated by SDS-PAGE and electrotransferred to polyvinylidene fluoride membranes and immunoblotted with anti-LDH-A (Abcam) or anti-FH (Novus) antibody for overnight at 4°C. After washing with TBS-Tween 20, the membrane was incubated with secondary antibody of choice for 30 min. The protein bands were detected using SuperSignal West Pico Chemiluminescent substrate (Pierce). For generation of FH/LDH-A clones, A549 cells were infected with FH and LDH-A shRNA and selected with puromycin and validated with Western blot analysis with FH and LDH-A antibodies for double knockdown. For tumor implantation, double stable FH/LDH-A cells were generated by larger-scale infection and tested for the lack of FH/LDH-A expression before implantation. LDH-A-deficient RCC4 cells were generated in a similar manner as described above and validated for LDH-A inhibition by Western blot analysis.

Proliferation Assay

Control, FH-deficient, and FH/LDH-A-deficient cell lines were plated in 60 mm dish at a density of 1×10^5 per dish in Ham's F-12 supplemented with 10% fetal bovine serum for 24 h at 37°C in a 5% CO_2 incubator. After 24, 48, 72, 96, and 120 h initial plating, cells were scraped, washed with PBS, and resuspended in 1 mL HBSS and counted in the presence of trypan blue. All samples were assayed in duplicate to generate proliferation curves as described (21).

Lactate Accumulation

We measured lactate accumulation in control and LDH-A-deficient cell lines as described (22). Briefly, the cell culture conditioned supernatant was used to measure lactate levels by a simple calorimetric analysis based on the reduction of the tetrazolium salt INT in a NADH-coupled enzymatic reaction to formazan, which is water-soluble and exhibits an absorption maximum at 492 nm. The intensity of the red color formed is proportional to the lactate concentration in the conditioned medium. All samples were assayed in three independent experiments in triplicate. The average value of the absorption readings was used for graphical representation.

LDH-A Enzyme Activity

LDH-A activity was measured in the direction of reduction of pyruvate to lactate by monitoring the changes in the absorbance of NADH at 340 nm. Briefly, the reaction mixture contained 50 mmol/L potassium phosphate (pH 7.4) and pyruvate (200 μmol/L). The reaction was initiated by addition of cell extract prepared in potassium phosphate and NADH (250 μmol/L), and decrease in absorbance at 340 nm was monitored every 4 min.

Intracellular ATP Measurements

Intracellular ATP levels in control, FH-deficient, and FH/LDH-A-deficient cells were measured according to the manufacturer's instructions and as described before (7). In brief, cell lysates were collected and luminescence was measured using a luminescence reader (Molecular Devices) and normalized for protein concentration.

Annexin V Apoptosis Assay

Apoptosis was measured by Guava PCA-96 Nexin (Guava Technologies) as per the manufacturer's protocol. Briefly, cells were harvested and resuspended in 1× Nexin buffer with Annexin V-PE and Nexin 7-amino-actinomycin D. The cells were allowed to incubate for 15 min and analyzed in the Guava flow cytometer.

Invasion Assay

The invasiveness of cells was analyzed using Falcon BioCoat Matrigel chambers (Becton Dickinson) with 6.4 mm diameter and 8 μm pore size. Invasiveness of cells expressing control, FH, and FH/LDH-A shRNA was assayed as described previously (23, 24). Briefly, 4×10^4 cells were seeded on the upper side of a Matrigel invasion chamber. After 24 h, the cells on the upper surface of the filter were removed using cotton swabs, and the invaded cells were fixed with 20% solution of 4% paraformaldehyde and stained with crystal violet. Incorporated dye was extracted with 0.05 mol/L sodium phosphate (pH 4.5) in 50% ethanol and the absorbance of released dye was read at 550 nm. The data represent average of two independent experiments done in triplicate.

Oxygen Consumption and Extracellular Acidification Rate Analysis

The XF24 extracellular flux analyzer (Seahorse Biosciences) is a fully integrated 24-well instrument that measures in real-time the uptake and release of metabolic end-products. Each XF24 assay well contains a disposable sensor cartridge, embedded with 24 pairs of fluorescent biosensors (oxygen and pH), coupled to fiber-optic waveguides. The wave guides deliver light ray at various excitation wavelengths (oxygen = 532 nm, pH = 470 nm) and transmit a fluorescent signal (oxygen = 650 nm, pH = 530 nm) to a set of highly sensitive photodetectors. This technology was used to measure oxygen consumption expressed in pmol/min and extracellular acidification rate, expressed in mpH/min in control, FH- and FH/LDH-A-deficient cell lines as described (25).

Reactive Oxygen Species Measurements

Intracellular reactive oxygen species (ROS) production was measured by staining with 2′,7′-dichlorodihydrofluorescein diacetate (H_2DCFDA; Invitrogen). H_2DCFDA is a cell-permeant indicator for ROS that is nonfluorescent until removal of the acetate groups by intracellular esterases and oxidation occurs within the cell. The procedure for measuring ROS was carried out as described earlier (7), with minor modification. Briefly, cells were loaded with 5 μmol/L H_2DCFDA for 1 h, washed in PBS, and incubated in fresh medium for 30 min. The cells were then subjected to fluorescence-activated cell sorting analysis to visualize the fluorescence.

Tumor Implantation

Control and FH65/LDH-A-deficient cells (3.0×10^6) were s.c. implanted in eight athymic mice. The implantation was done such that each mouse had FH65 cells on the right flank and FH65/LDH-A-deficient cells on the left flank. The control shRNA cells were implanted in a separate set of athymic mice. Tumors were measured every 5 days and tumor volume was calculated as described before (26). Tumor lysates were prepared by homogenization of tumor tissues in lysis buffer, separated by SDS-PAGE, electrotransferred to polyvinylidene fluoride membranes, immunoblotted with anti-LDH-A and anti-FH antibody, and normalized by actin as a loading control.

Statistical Analysis

Student's *t* test was used to evaluate the statistical significance of the results.

Results

Enhanced Expression of LDH-A in HLRCC

Because FH deficiency up-regulates HIF-1α (13), and LDH-A is a known HIF-1α target, we asked whether expression of LDH-A is significantly enhanced in HLRCC tumors. Previous microarray profiling data in FH-deficient uterine fibroids suggest that LDH-A expression may be increased compared with normal myometrium (27). As

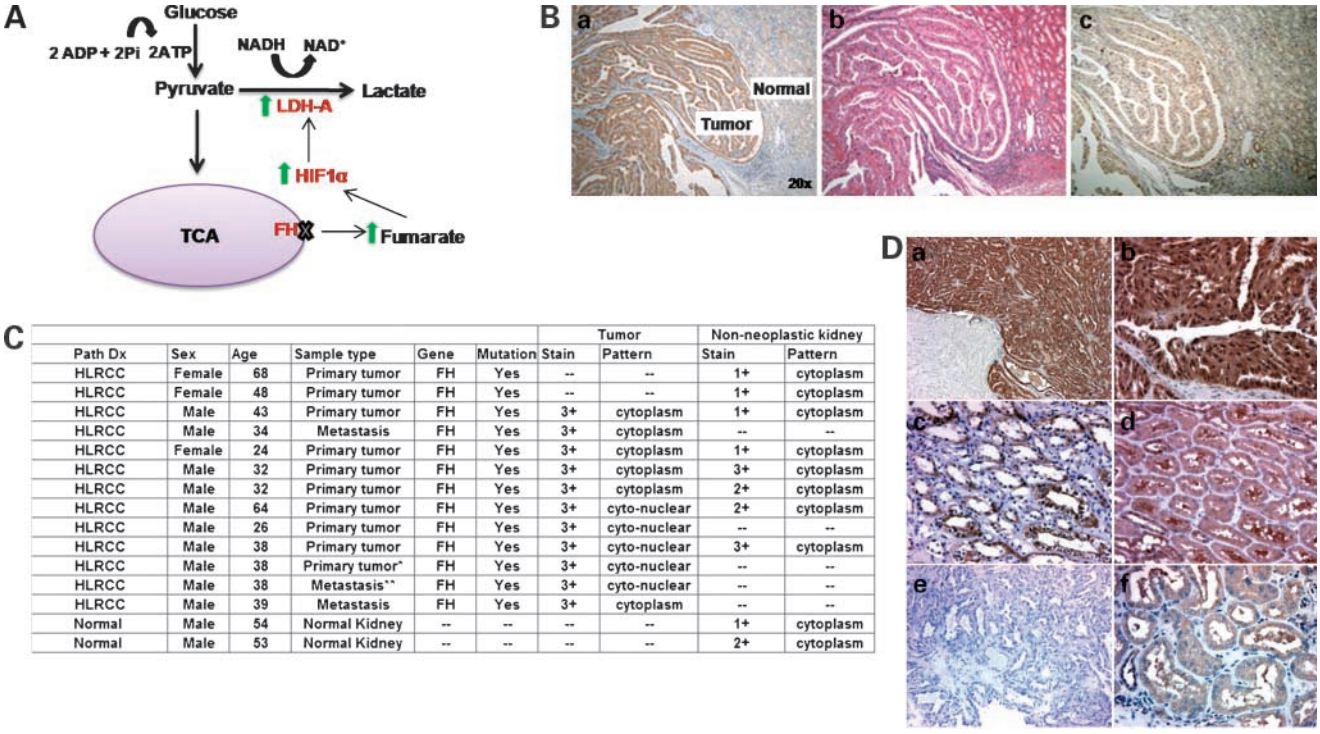

C

						Tumor		Non-neoplastic kidney	
Path Dx	Sex	Age	Sample type	Gene	Mutation	Stain	Pattern	Stain	Pattern
HLRCC	Female	68	Primary tumor	FH	Yes	--	--	1+	cytoplasm
HLRCC	Female	48	Primary tumor	FH	Yes	--	--	1+	cytoplasm
HLRCC	Male	43	Primary tumor	FH	Yes	3+	cytoplasm	1+	cytoplasm
HLRCC	Male	34	Metastasis	FH	Yes	3+	cytoplasm	--	--
HLRCC	Female	24	Primary tumor	FH	Yes	3+	cytoplasm	1+	cytoplasm
HLRCC	Male	32	Primary tumor	FH	Yes	3+	cytoplasm	3+	cytoplasm
HLRCC	Male	32	Primary tumor	FH	Yes	3+	cytoplasm	2+	cytoplasm
HLRCC	Male	64	Primary tumor	FH	Yes	3+	cyto-nuclear	2+	cytoplasm
HLRCC	Male	26	Primary tumor	FH	Yes	3+	cyto-nuclear	--	--
HLRCC	Male	38	Primary tumor	FH	Yes	3+	cyto-nuclear	3+	cytoplasm
HLRCC	Male	38	Primary tumor*	FH	Yes	3+	cyto-nuclear	--	--
HLRCC	Male	38	Metastasis**	FH	Yes	3+	cyto-nuclear	--	--
HLRCC	Male	39	Metastasis	FH	Yes	3+	cytoplasm	--	--
Normal	Male	54	Normal Kidney	--	--	--	--	1+	cytoplasm
Normal	Male	53	Normal Kidney	--	--	--	--	2+	cytoplasm

Figure 1. LDH-A is overexpressed in HLRCC tumors. **A,** schematic representation of tricarboxylic acid/glycolysis pathways in HLRCC. FH deficiency results in increased HIF-1α expression resulting in enhanced LDH-A. **B,** increased expression of LDH-A in HLRCC tumor sample (**a**), H&E staining (**b**), and HIF-1α immunostaining (**c**) and on same tumor section. **C,** enhanced LDH-A staining in HLRCC tumor samples derived from HLRCC patients and sequence validated to confirm FH mutation compared with sporadic renal cancer with no detectable mutation in FH. **D,** representative LDH-A staining for the HLRCC cases. Most tumor cells stained strongly for LDH-A in the cytoplasm and nuclei (**a** and **b**). In the adjacent nonneoplastic kidney (treated as internal normal control), there was a heterogeneous staining pattern with some tubules having moderate or weak staining (**c** and **d**). Incubation of the samples with isotype-matched IgG (negative control) always resulted in no staining (**e**). Tubules from nonmalignant kidney derived from sporadic clear cell tumors stained weakly or moderately for LDH-A, and the staining was limited to the cytoplasm (**f**). *Asterisk,* second sample from same patient; *double asterisk,* metastatic sample from same patient.

shown in Fig. 1A, LDH-A expression is abundant in HLRCC tumors and almost negligible in surrounding normal tissue. This expression pattern largely overlaps with HIF expression in the corresponding section from the same tumor (Fig. 1B). This result is almost universal in HLRCC tumor samples that were sequence validated for FH mutations (Fig. 1C and D). Based on these results, we wanted to ask whether inhibition of LDH-A in a FH-deficient background would have significant effect on the survival or the rate of proliferation of FH-deficient cells *in vitro*.

Generation and Validation of FH-Deficient Cell Lines as a Surrogate Cell Culture Model for HLRCC

Because there is no established HLRCC cell line that can be used to study metabolic alterations and signaling events associated with FH deficiency, we used the A549 lung cancer cell line as a surrogate model system to generate FH-deficient cell lines. Our choice of the cell line to create HLRCC surrogate model system in cell culture was based on the previous publication that suggested that these cells carry wild-type VHL gene, as is the case in HLRCC patients, and inhibition of endogenous FH expression in these cells results in enhanced glycolysis (13). Western blot analysis with anti-FH antibody shows that cell lines FH63 and FH65, which express shRNAs targeting two different regions within the FH mRNA, have diminished FH protein expression compared with the cell line expressing control shRNA (Fig. 2A). The FH-deficient cells compared with control cells have comparable rates of proliferation (Fig. 2B). However, in agreement with the study by Isaacs et al. (14), FH-deficient cells compared with control cells have increased lactate levels (Fig. 2C), enhanced HIF-1α expression in normoxic conditions (Fig. 2F), and showed increased expression of two HIF-1α target genes, GLUT1 and vascular endothelial growth factor (VEGF; Fig. 2D and E). Because FH deficiency mimics the pseudohypoxic state that should favor fermentative glycolysis regulated by LDH-A, a HIF-1α target, we also found increased HIF-1α expression in FH-deficient cells and a 2.0-fold increase in LDH-A enzyme activity in FH-deficient cells compared with empty vector control or wild-type cells as measured by loss of NADH in the presence of pyruvate (Fig. 2G).

Generation and Validation of LDH-A-Deficient Cell Lines in a FH-Deficient Background

To test whether inhibition of LDH-A in FH-deficient cells would result in reduced proliferation, we generated

LDH-A-deficient cells in a FH-deficient background and will refer to these cells as FH/LDH-A-deficient cells in this article. Western blot analysis with anti-FH and anti-LDH-A antibodies shows that cell lines FH63/LDH-A and FH65/LDH-A have diminished FH and LDH-A protein expression compared with the control cell line or FH only-deficient cell lines (Fig. 3A and B). As expected, FH65 shRNA cells show increased lactate formation as measured by lactate accumulation and real-time measurements in a XF-24 metabolite analyzer compared with control cells, but FH/LDH-A-deficient cells show reduced lactate formation (Fig. 3C and D).

In vitro Characterization of FH/LDH-A-Deficient Cell Lines

Next, we asked whether cell lines deficient in FH/LDH-A expression would show altered cell survival/growth. We first characterized these stable cell lines in various *in vitro* assays. As shown in Fig. 4A, all FH/LDH-A-deficient cell lines display a significant proliferation defect compared with cells with LDH-A knockdown in the background of wild-type FH gene. The FH/LDH-A-deficient cells also show significantly higher levels of apoptosis compared with control shRNA cells (Fig. 4B). Moreover, induction of apoptosis is also shown by Western blot analysis of caspase-3 cleavage and PARP cleavage in FH/LDH-A-deficient cell lines (Fig. 4C). These data could also be extended to growth in three dimensions: we have noted that, in a soft agar growth assay, LDH-A-deficient cells on a FH-deficient background generate smaller colonies compared with FH-deficient cells, suggesting lower tumorigenic potential (data not shown).

As metastatic potential is one of the hallmarks of HLRCC tumors (28, 29), we asked whether a cell line deficient in FH would display a more invasive phenotype as assessed by a Matrigel invasion assay. We found that FH-deficient cells have significantly enhanced invasive potential in this assay and this invasive behavior can be dialed back to the same level as cells expressing control shRNA (Fig. 3E) by LDH-A inhibition. Moreover, this invasive ability correlated with lactic acid generation (Fig. 3C and D).

To determine the effect on ATP generation of LDH-A inhibition in FH-deficient cells, ATP levels were measured. In comparison with the control cells or FH alone-deficient cells, FH/LDH-A-deficient cells show significant ATP depletion (~50-60% reduction; Fig. 5A). This result is in agreement with the substantially reduced proliferation rate

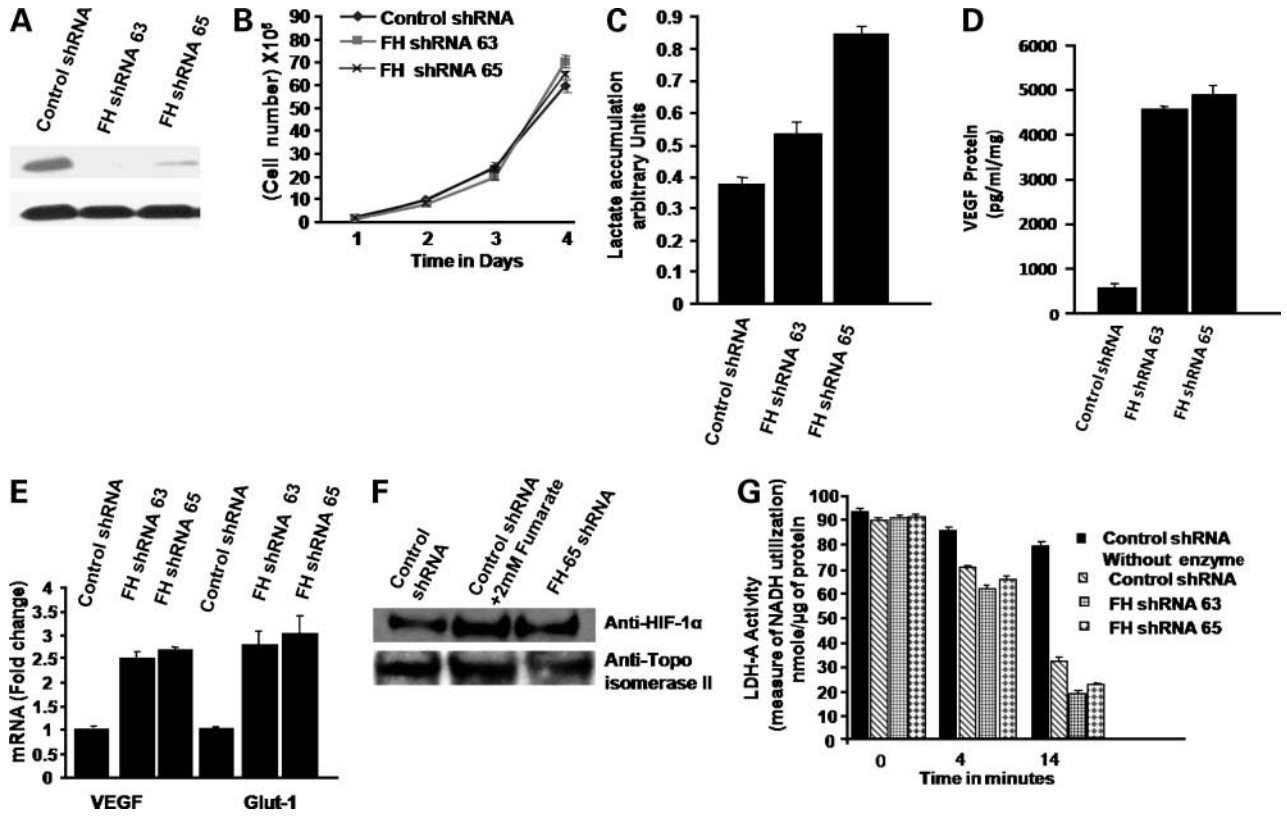

Figure 2. Characterization of FH-deficient cell lines. **A,** Western blot analysis of control shRNA cell line, FH63 shRNA, and FH65 shRNA cell lines by anti-FH and anti-LDH-A antibody. **B,** proliferation assay analysis of control shRNA cell line, FH63 shRNA, and FH65 shRNA cell lines. **C,** lactate measurement in control and A549 FH-deficient cell lines. Mean of three independent experiments done in duplicate ($P < 0.004$). **D,** VEGF measurement in control and A549 FH-deficient cell lines. Mean of three independents experiment done in duplicate ($P < 0.005$). **E,** real-time PCR analysis of VEGF and GLUT1 in the FH63 shRNA and FH65 shRNA cell lines. **F,** HIF-1α expression in control shRNA cell line, FH65 shRNA cell line, and control shRNA cells in the presence of 2.0 mmol/L fumarate (ester derivative) as positive control. **G,** mean LDH-A activity in FH-deficient cell lines. Mean of three independent experiments done in duplicate ($P < 0.05$).

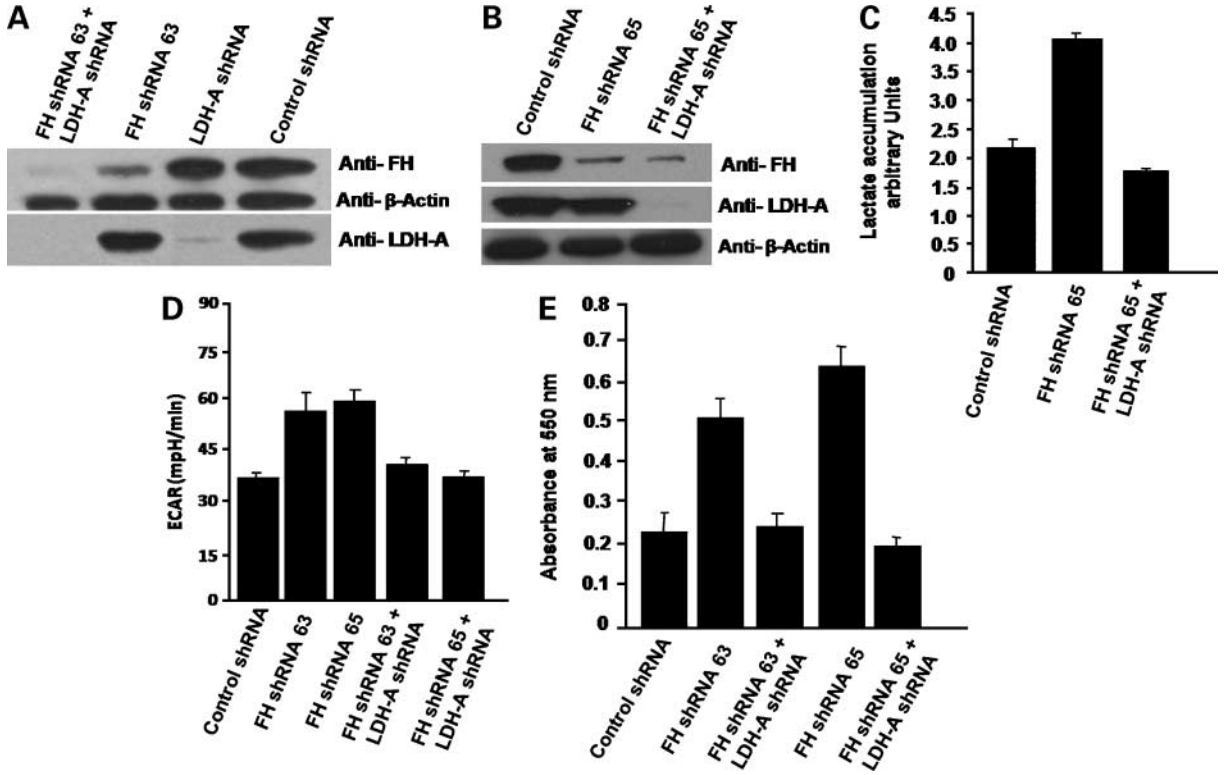

Figure 3. Characterization of FH/LDH-A-deficient cells. **A** and **B,** Western blot analysis of LDH-A/FH-deficient A549 cell lines by anti-LDH-A or anti-FH antibody. **C,** lactate accumulation and measurements in FH-deficient cells and FH/LDH-A cell lines. Mean of two independent experiments done in duplicate. **D,** extracellular acidification rate as a measure of lactic acid production in control, FH-deficient, and FH/LDH-A-deficient cells. Mean of two independent experiments done in duplicate ($P < 0.05$). **E,** rate of invasion through Matrigel in control, FH-deficient, and FH/LDH-A-deficient cell lines. Mean of two independent experiments done in triplicate.

observed in our various growth assays. We were unable to show increased NADH/NAD^+ ratio (data not shown) in FH/LDH-A-deficient cells. Furthermore, we also noted an increased rate of oxygen consumption in FH/LDH-A-deficient cells, suggesting that LDH-A inhibition in FH-deficient background may be forcing the cells to increase oxidative phosphorylation (Fig. 5B).

Enhanced LDH-A Expression Occurs in Renal Tumors with VHL Deficiency

VHL deficiency is a common feature of clear cell renal carcinoma (30, 31). It also results in HIF-1α up-regulation (32). We would therefore expect enhanced LDH-A expression in VHL-deficient renal cancer tumor tissue samples. This was indeed found to be the case (Fig. 6A). Moreover, we have also shown that inhibition of LDH-A by two different shRNAs in the VHL-deficient cell line RCC4 results in increased apoptosis (Fig. 6B and C). RCC4 cells reconstituted with wild-type VHL lacks LDH-A expression as a result of diminished HIF-1α expression (33); hence, these cells cannot be used to generate LDH-A-deficient cell lines for comparison studies between VHL-deficient and VHL-reconstituted RCC4 cells. Our analysis of VHL-deficient tumors and *in vitro* data suggest that LDH-A is overexpressed in VHL-deficient cells and its inhibition results in apoptosis.

Increased ROS Generation in FH/LDH-A-Deficient Cells Correlates with Apoptosis

Based on our previous results, we asked whether enhanced oxidative phosphorylation due to LDH-A knockdown in FH-deficient cells might result in increased formation of ROS. H_2DCFDA is a fluorogenic probe commonly used to detect cellular ROS. We found enhanced ROS levels as measured by H_2DCFDA in FH/LDH-A-deficient cells compared with control or FH-deficient cells (Fig. 5C). Furthermore, this ROS generation could be blocked by the antioxidant *N*-acetylcysteine and resulted in partial rescues from apoptosis as measured by cleaved PARP (Fig. 5D). These data suggest that ROS generation may be partly implicated in the increased apoptosis seen in FH/LDH-A-deficient cells.

In vivo Characterization of FH/LDH-A-Deficient Cell Lines

To ask whether FH/LDH-A-deficient cell lines have significantly diminished potential for tumor formation, we implanted these cells into the flanks of athymic mice. We found that FH65/LDH-A knockdown cells show marked growth inhibition (Fig. 7A) compared with cells expressing control or FH shRNA. We also show representative tumor tissue from control, FH-deficient, and FH/LDH-A-deficient tumors assayed for FH and LDH-A

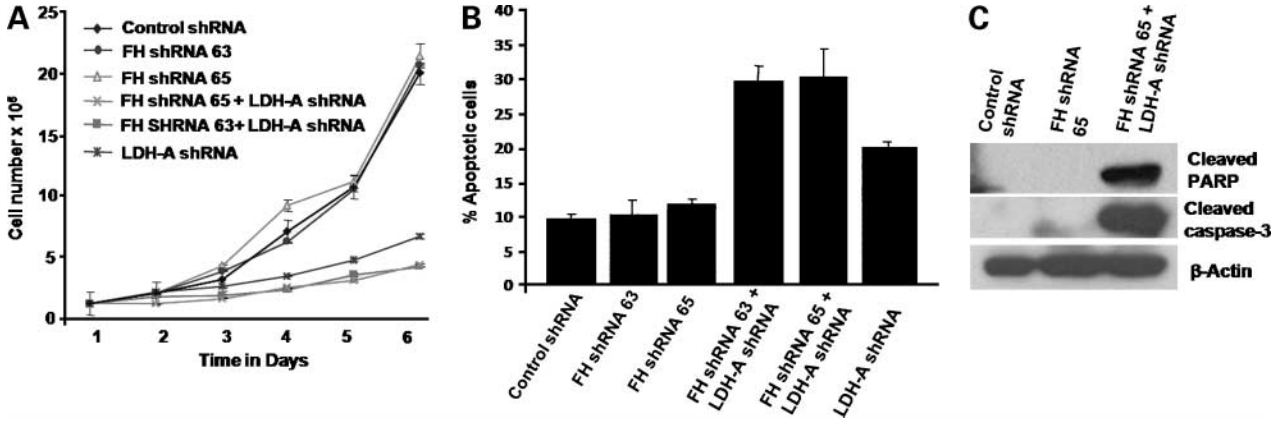

Figure 4. FH/LDH-A-deficient cell lines have diminished proliferation rate. **A,** proliferation assay to measure rate of growth in cells expressing control, FH, LDH-A, and FH/LDH-A shRNA. **B,** apoptosis analysis of FH/LDH-A-deficient A549 cell lines with Annexin V-PE with Guava flow cytometer. Mean of three independent experiments done in duplicate ($P < 0.005$). **C,** Western blot analysis of cleaved PARP and cleaved caspase-3 in cells expressing control, FH, and FH/LDH-A shRNA.

expression (Fig. 7B) to confirm that tumor cells *in vivo* displayed diminished expression of FH and LDH-A as they had *in vitro*. These results are similar to those recently published by Fantin et al. (34).

Discussion

The major findings in this report are the following: (*a*) HLRCC tumors overexpress LDH-A, (*b*) LDH-A inhibition results in increased apoptosis via ROS production in an A549 surrogate FH knockdown cell line, and (*c*) inhibition of fermentative glycolysis in this cell line results in significant reduction in growth in a xenograft mouse model.

The common feature of tumor cells is their reliance on fermentative glycolysis, a phenomenon coined as the Warburg effect (1). Although the mechanism that may control this metabolic shift is not clearly defined, many

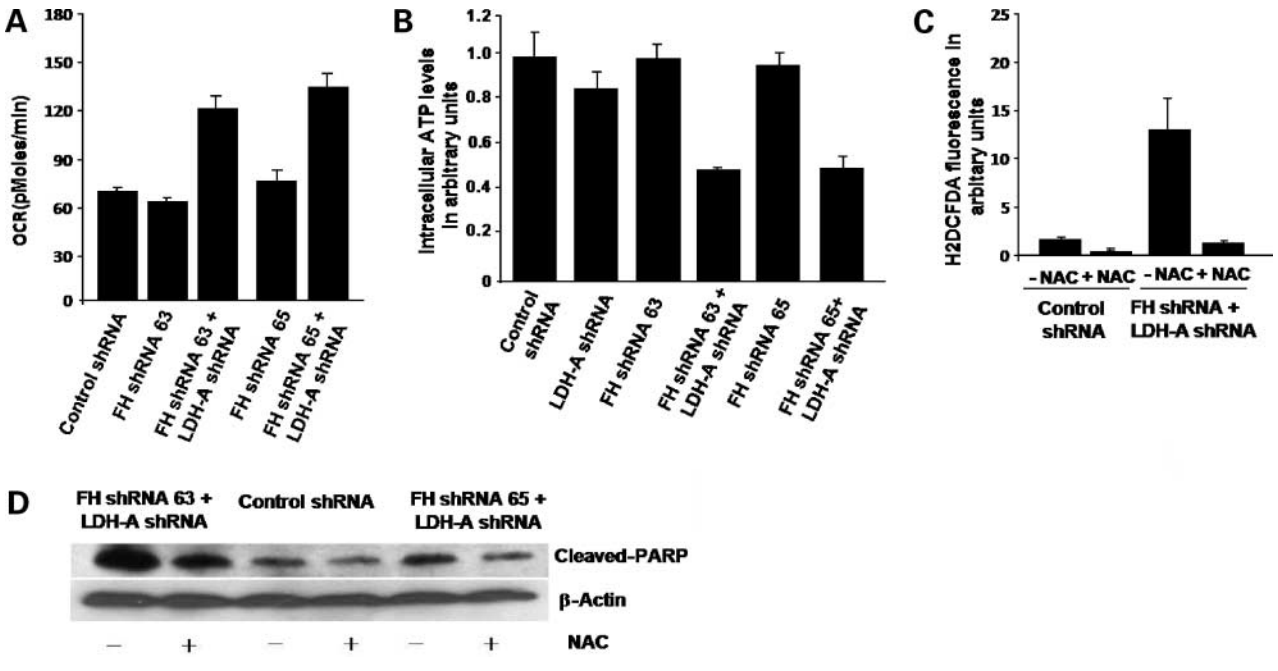

Figure 5. Metabolic effect of LDH-A inhibition in FH-deficient background. **A,** oxygen consumption measurement by XF24 extracellular flux analysis rate in control, FH-deficient, and FH/LDH-A-deficient cells. Three independent experiments done in triplicate ($P > 0.05$). **B,** intracellular ATP in control, LDH-A-deficient, and FH/LDH-A-deficient cells. **C,** ROS measurement by H_2DCFDA in control and FH/LDH-A-deficient cell lines in the presence and absence of *N*-acetylcysteine. Mean of two independent experiments done in duplicate ($P < 0.05$). **D,** Western blot analysis of cleaved PARP in control, FH-deficient, and FH/LDH-A-deficient cells in the presence and absence of 5 mmol/L *N*-acetylcysteine.

A

						Tumor		Non-neoplastic kidney	
Path Dx	Sex	Age	Sample type	Gene	Mutation	Stain	Pattern	Stain	Pattern
Clear Cell	Female	28	Primary tumor	VHL	Yes	3+	cytoplasm	2+	cytoplasm
Clear Cell	Female	69	Primary tumor	VHL	Yes	3+	cytoplasm	--	--
Clear Cell	Female	34	Primary tumor	VHL	Yes	3+	cytoplasm	--	--
Clear Cell	Male	56	Primary tumor	VHL	Yes	3+	cytoplasm	--	--
Clear Cell	Male	36	Primary tumor	VHL	Yes	2+	cytoplasm	1+	cytoplasm
Clear Cell	Female	51	Primary tumor	VHL	Yes	2+	cytoplasm	1+	cytoplasm
Normal	Male	54	Normal Kidney	--	--	--	--	1+	cytoplasm

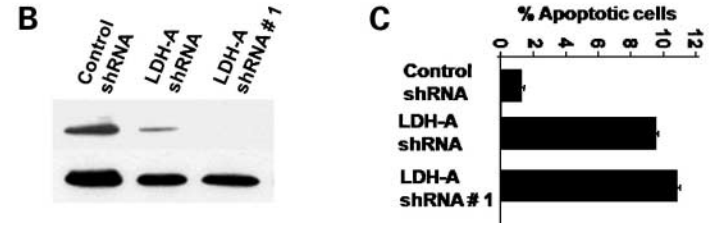

Figure 6. Enhanced LDH-A expression in VHL-deficient tumors. **A,** enhanced LDH-A expression as assessed by immunohistochemical staining in tumor samples derived from clear cell carcinoma patients and sequence validated to confirm VHL mutation compared with LDH-A staining in nonmalignant kidney tissue, designated as normal. **B,** Western blot analysis of LDH-A-deficient RCC4 (VHL null) cells by anti-LDH-A antibody. **C,** apoptosis analysis of RCC4 cells expressing control shRNA and LDH-A-deficient RCC4 cells with Annexin V-PE with Guava flow cytometer. Mean of three independent experiments done in duplicate ($P < 0.005$).

lines of investigations suggest that HIF expression may be central to Warburg effect both by induction of fermentative glycolysis and by diminishing the activity of pyruvate dehydrogenase (7, 8). FH inactivation should mimic this state, as it results in increased expression of HIF-1α and up-regulation of HIF-dependent glycolysis (13, 35). This pseudohypoxic drive is similar to that described in VHL-deficient cells as a result of the HIF accumulation in the absence of the appropriate ubiquitination process that targets HIF. The switch to the fermentative glycolysis should therefore be a common feature in tumors with VHL, FH, and succinate dehydrogenase deficiency, resulting from HIF-1α stabilization, and we would expect to see increased LDH-A expression in these tumors. Indeed, we have shown this to be the case in two of these tumor types (VHL- and FH-deficient tumors).

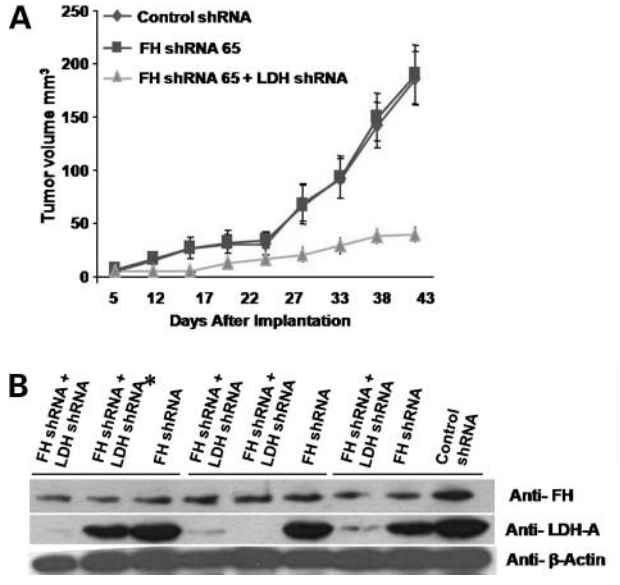

Figure 7. *In vivo* characterization of FH/LDH-A-deficient cells. **A,** LDH-A knockdown in FH-deficient cells results in reduced tumor growth. **B,** Western blot analysis of representative tumor tissue with FH and LDH-A antibodies. *Tumor set taken out of the analysis.

The functional consequences of inhibiting LDH-A have been explored both *in vitro* and *in vivo*. In the background of FH deficiency, LDH-A knockdown cells proliferate slower, undergo apoptosis, and are less invasive. The underlying basis for these effects remains to be fully defined. FH/LDH-A-deficient cells did show ~50% to 60% reduction in intracellular ATP. We were surprised that the levels were not more profoundly depressed because both fermentative glycolysis and tricarboxylic acid cycle were expected to be compromised in FH/LDH-A cells. It is possible that intracellular ATP levels are being sustained by leakiness in our surrogate system, by LDH-B overactivity or expression compensating for LDH-A inhibition, or by diminished ATP consumption. We are currently exploring whether inhibition of both isoforms of LDH may result in significant ATP depletion. This might be technically challenging, as it will involve a triple knockdown to create such a cell line.

A correlation among apoptosis, ROS, and mitochondrial respiration has been reported in several cancers (36). Studies have suggested that HIF-1α-dependent mitochondrial repression may provide survival benefit by decreasing the risk associated with apoptotic cell death (37). Moreover, reduced ROS levels and decreased apoptosis result from forced expression of HIF-1α in oral squamous cell carcinoma (38). We therefore asked if increased ROS production was mediating apoptosis. This appears to be

the case, at least partially, because *N*-acetylcysteine was able to decrease PARP cleavage. We also found that oxidative phosphorylation was enhanced in FH/LDH-deficient cells as evidenced by increased oxygen consumption. One effect of this might be to increase electron flow in oxidative phosphorylation and thereby account for increased ROS production. However, in preliminary observations, we did not find increased superoxide formation as measured by the Mitosox reagent (data not shown), so the source of increased ROS production remains to be defined. It is also possible that various antioxidant systems in these cells have also been affected accounting for increased ROS.

Another effect of the increased rate of oxygen consumption observed in FH/LDH-A-deficient cells could be to maintain the $NADH/NAD^+$ ratio. Because LDH-A catalyzes regeneration of NAD^+ from NADH, we expected to observe an increased $NADH/NAD^+$ ratio in FH/LDH-deficient cells. The competitive phenomenon between mitochondrial $NADH/NAD^+$ transport system and LDH-A for NADH consumption is driven by LDH-A as a result of its fast enzymatic kinetic properties and is thought to be a potential factor for decreased mitochondrial respiration (39). Our failure to note an increase in the $NADH/NAD^+$ ratio may be partly due to a decrease in the LDH-A-driven competitive reaction that drives more NADH into mitochondria.

Because hypoxia regulates transcription factors HIF-1 and HIF-2, and in general it is difficult to design inhibitors targeting transcription factors, we have investigated whether targeting downstream targets of HIF-1 and HIF-2 may be therapeutically advantageous. Indeed, VEGF, a HIF-1α-induced gene product, has been successfully targeted for renal cell carcinoma therapy and our *in vitro* data showing enhanced VEGF expression in these cells supports the use of VEGF inhibitors in HLRCC. Our *in vitro* and *in vivo* data support the notion that targeting LDH-A, another HIF-1α target, may be a viable strategy for treating this disease as well. Moreover, high lactate levels are associated with poor prognosis in advanced renal cell carcinoma (40) and head and neck cancer (41). It is likely that inhibition of LDH-A by increasing the extracellular pH (42, 43) may reduce the metastatic ability of these advanced cancer cells as extrapolated from our *in vitro* invasion assay results. Also, HLRCC patients may benefit from combined antiangiogenic and LDH-A inhibitor therapy as might patients with any tumors that have up-regulated HIF.

Our findings add to a growing literature that suggest that metabolism plays a key role in tumorigenesis and is linked either directly or indirectly to hallmarks of cancer that are involved in initiation and proliferation of tumors. In conclusion, our data support the hypothesis that inhibition of fermentative glycolysis might serve as a therapeutic strategy for HLRCC. Therefore, the development of inhibitors of LDH-A makes eminent sense for the treatment of HLRCC and a potentially large group of cancers in which the Warburg effect is operational, perhaps as many as 60% to 80% of tumor types.

Disclosure of Potential Conflicts of Interest

No potential conflicts of interest were disclosed.

References

1. Gatenby RA, Gillies RJ. Why do cancers have high aerobic glycolysis? Nat Rev Cancer 2004;4:891 – 9.

2. Iyer NV, Kotch LE, Agani F, et al. Cellular and developmental control of O_2 homeostasis by hypoxia-inducible factor 1α. Genes Dev 1998;12: 149 – 62.

3. Robey IF, Lien AD, Welsh SJ, Baggett BK, Gillies RJ. Hypoxia-inducible factor-1α and the glycolytic phenotype in tumors. Neoplasia 2005;7: 324 – 30.

4. Seagroves TN, Ryan HE, Lu H, et al. Transcription factor HIF-1 is a necessary mediator of the Pasteur effect in mammalian cells. Mol Cell Biol 2001;21:3436 – 44.

5. Semenza GL, Roth PH, Fang HM, Wang GL. Transcriptional regulation of genes encoding glycolytic enzymes by hypoxia-inducible factor 1. J Biol Chem 1994;269:23757 – 63.

6. Semenza GL, Rue EA, Iyer NV, Pang MG, Kearns WG. Assignment of the hypoxia-inducible factor 1α gene to a region of conserved synteny on mouse chromosome 12 and human chromosome 14q. Genomics 1996; 34:437 – 9.

7. Kim JW, Tchernyshyov I, Semenza GL, Dang CV. HIF-1-mediated expression of pyruvate dehydrogenase kinase: a metabolic switch required for cellular adaptation to hypoxia. Cell Metab 2006;3:177 – 85.

8. Papandreou I, Cairns RA, Fontana L, Lim AL, Denko NC. HIF-1 mediates adaptation to hypoxia by actively downregulating mitochondrial oxygen consumption. Cell Metab 2006;3:187 – 97.

9. Warburg O. The metabolism of tumors. London: Arnold Constable; 1930.

10. Kiuru M, Launonen V, Hietala M, et al. Familial cutaneous leiomyomatosis is a two-hit condition associated with renal cell cancer of characteristic histopathology. Am J Pathol 2001;159:825 – 9.

11. Tomlinson IP, Alam NA, Rowan AJ, et al. Germline mutations in FH predispose to dominantly inherited uterine fibroids, skin leiomyomata and papillary renal cell cancer. Nat Genet 2002;30:406 – 10.

12. Toro JR, Nickerson ML, Wei MH, et al. Mutations in the fumarate hydratase gene cause hereditary leiomyomatosis and renal cell cancer in families in North America. Am J Hum Genet 2003;73:95 – 106.

13. Isaacs JS, Jung YJ, Mole DR, et al. HIF overexpression correlates with biallelic loss of fumarate hydratase in renal cancer: novel role of fumarate in regulation of HIF stability. Cancer Cell 2005;8:143 – 53.

14. Rodriguez S, Jafer O, Goker H, et al. Expression profile of genes from 12p in testicular germ cell tumors of adolescents and adults associated with i(12p) and amplification at 12p11.2-p12.1. Oncogene 2003;22: 1880 – 91.

15. Zhong H, De Marzo AM, Laughner E, et al. Overexpression of hypoxia-inducible factor 1α in common human cancers and their metastases. Cancer Res 1999;59:5830 – 5.

16. Kanno T, Sudo K, Maekawa M, Nishimura Y, Ukita M, Fukutake K. Lactate dehydrogenase M-subunit deficiency: a new type of hereditary exertional myopathy. Clin Chim Acta 1988;173:89 – 98.

17. Kanno T, Sudo K, Takeuchi I, et al. Hereditary deficiency of lactate dehydrogenase M-subunit. Clin Chim Acta 1980;108:267 – 76.

18. Kanno T, Sudo K, Kitamura M, Miwa S, Ichiyama A, Nishimura Y. Lactate dehydrogenase A-subunit and B-subunit deficiencies: comparison of the physiological roles of LDH isozymes. Isozymes Curr Top Biol Med Res 1983;7:131 – 50.

19. Miwa S, Nishina T, Kakehashi J, Kitamura M. Hereditary H type LDH deficiency. 2. Abnormal glycolytic metabolism in the erythrocyte. Rinsho Byori 1971;19 Suppl:371.

20. Root DE, Hacohen N, Hahn WC, Lander ES, Sabatini DM. Genome-scale loss-of-function screening with a lentiviral RNAi library. Nat Methods 2006;3:715 – 9.

21. Benson JD, Chen YN, Cornell-Kennon SA, et al. Validating cancer drug targets. Nature 2006;441:451 – 6.

22. Lu H, Forbes RA, Verma A. Hypoxia-inducible factor 1 activation by aerobic glycolysis implicates the Warburg effect in carcinogenesis. J Biol Chem 2002;277:23111 – 5.

23. Saito K, Oku T, Ata N, Miyashiro H, Hattori M, Saiki I. A modified and convenient method for assessing tumor cell invasion and migration and its application to screening for inhibitors. Biol Pharm Bull 1997;20:345 – 8.

24. Schreiner A, Ruonala M, Jakob V, et al. Junction protein shrew-1 influences cell invasion and interacts with invasion-promoting protein CD147. Mol Biol Cell 2007;18:1272 – 81.

25. Wu M, Neilson A, Swift AL, et al. Multiparameter metabolic analysis reveals a close link between attenuated mitochondrial bioenergetic function and enhanced glycolysis dependency in human tumor cells. Am J Physiol Cell Physiol 2007;292:C125 – 36.

26. Ananth S, Knebelmann B, Gruning W, et al. Transforming growth factor beta1 is a target for the von Hippel-Lindau tumor suppressor and a critical growth factor for clear cell renal carcinoma. Cancer Res 1999;59: 2210 – 6.

27. Vanharanta S, Pollard PJ, Lehtonen HJ, et al. Distinct expression profile in fumarate-hydratase-deficient uterine fibroids. Hum Mol Genet 2006;15:97 – 103.

28. Grubb RL III, Franks ME, Toro J, et al. Hereditary leiomyomatosis and renal cell cancer: a syndrome associated with an aggressive form of inherited renal cancer. J Urol 2007;177:2074 – 9; discussion 2079 – 2080.

29. Sudarshan S, Linehan WM. Genetic basis of cancer of the kidney. Semin Oncol 2006;33:544 – 51.

30. Gnarra JR, Tory K, Weng Y, et al. Mutations of the VHL tumour suppressor gene in renal carcinoma. Nat Genet 1994;7:85 – 90.

31. Linehan WM, Lerman MI, Zbar B. Identification of the von Hippel-Lindau (VHL) gene. Its role in renal cancer. JAMA 1995;273:564 – 70.

32. Mandriota SJ, Turner KJ, Davies DR, et al. HIF activation identifies early lesions in VHL kidneys: evidence for site-specific tumor suppressor function in the nephron. Cancer Cell 2002;1:459 – 68.

33. Hu CJ, Wang LY, Chodosh LA, Keith B, Simon MC. Differential roles of hypoxia-inducible factor 1α (HIF-1α) and HIF-2α in hypoxic gene regulation. Mol Cell Biol 2003;23:9361 – 74.

34. Fantin VR, St-Pierre J, Leder P. Attenuation of LDH-A expression uncovers a link between glycolysis, mitochondrial physiology, and tumor maintenance. Cancer Cell 2006;9:425 – 34.

35. Sudarshan S, Linehan WM, Neckers L. HIF and fumarate hydratase in renal cancer. Br J Cancer 2007;96:403 – 7.

36. Santamaria G, Martinez-Diez M, Fabregat I, Cuezva JM. Efficient execution of cell death in non-glycolytic cells requires the generation of ROS controlled by the activity of mitochondrial H^+-ATP synthase. Carcinogenesis 2006;27:925 – 35.

37. Zhang H, Gao P, Fukuda R, et al. HIF-1 inhibits mitochondrial biogenesis and cellular respiration in VHL-deficient renal cell carcinoma by repression of C-MYC activity. Cancer Cell 2007;11:407 – 20.

38. Sasabe E, Tatemoto Y, Li D, Yamamoto T, Osaki T. Mechanism of HIF-1α-dependent suppression of hypoxia-induced apoptosis in squamous cell carcinoma cells. Cancer Sci 2005;96:394 – 402.

39. Golshani-Hebroni SG, Bessman SP. Hexokinase binding to mitochondria: a basis for proliferative energy metabolism. J Bioenerg Biomembr 1997;29:331 – 8.

40. Motzer RJ, Bacik J, Mazumdar M. Prognostic factors for survival of patients with stage IV renal cell carcinoma: Memorial Sloan-Kettering Cancer Center experience. Clin Cancer Res 2004;10:6302 – 3S.

41. Brizel DM, Schroeder T, Scher RL, et al. Elevated tumor lactate concentrations predict for an increased risk of metastases in head-and-neck cancer. Int J Radiat Oncol Biol Phys 2001;51:349 – 53.

42. Gillies RJ. The tumour microenvironment: causes and consequences of hypoxia and acidity. Introduction. Novartis Found Symp 2001; 240:1 – 6.

43. Gillies RJ. Causes and consequences of hypoxia and acidity in tumors-Novartis Foundation symposium. Trends Mol Med 2001;7:47 – 9.